Silvio Rainho Teixeira, Maximina Romero, Jesus Ma. Rincón, Crystallization of SiO_2–CaO–Na_2O Glass Using Sugarcane Bagasse Ash as Silica Source. *Journal of the American Ceramic Society, 93 (2010) 450-455*; doi: 10.1111/j.1551-2916.2009.03431.x

Crystallization of SiO_2–CaO–Na_2O Glass Using Sugarcane Bagasse Ash as Silica Source

Silvio Rainho Teixeira[a], Maximina Romero[b], Jesus Ma. Rincón[b]

[a] Departamento Física, Química e Biologia, Universidade Estadual Paulista–UNESP, Presidente Prudente, SP 19060-080, Brazil

[b] Department of Building Construction Systems, Eduardo Torroja Institute for Construction Sciences-CSIC, 28033 Madrid, Spain

Abstract

This work reports the feasibility results of recycling sugar cane bagasse ash (SCBA) to produce glass–ceramic. The major component of this solid residue is SiO_2 (>89%). A 100 g batch composition containing ash, CaO and Na_2O was melted and afterward, poured into water to produce a glass frit. The crystallization kinetic study by nonisothermal method was performed on powder samples (<63 μm) at five different heating rates. Wollastonite is the major phase in crystallization at T>970°C, and below this temperature there is a predominance of rankinite. The crystallization activation energies calculated by the Kissinger and Ligero methods are equivalent: 374±10 and 378±13 kJ/mol. The growth morphology parameters have equal values n=m=1.5 indicating that bulk nucleation is the dominant mechanism in this crystallization process, where there is a three-dimensional growth of crystals with polyhedron-like morphology controlled by diffusion from a constant number of nuclei. However, differential thermal analysis (DTA) curves on both monolithic and powder glass samples suggest that crystallization of the powder glass sample occurs through a surface mechanism. The divergence in both results suggests that the early stage of surface crystallization occurs through a three-dimensional growth of crystals, which will then transform to one-dimensional growth.

I. Introduction

Industrial processes and energy production always produce waste. Nowadays, there is worldwide consensus that there is a need to recycle and reutilize these waste residues for an efficient utilization of natural resources. A wide variety of industrial residues have been used in the production of glass–ceramics.[1–6] Rawlings *et al.*[7] published a review on the re-use of residues containing silica for the production of glass–ceramics. The versatility of the process of

glass–ceramics production is manifested by the great number of residues that have been used as primary matter in its production: high furnace slag, fly ash from the burning of charcoal and garbage, sludge from galvanoplasty and alumina production, and remains of disposable glass, among other types. Published works have shown the potential of transforming silicate-based residues into glass–ceramic products of great utility. The general process involves the vitrification of a silicate (residue), or mixture of various residues, followed by a crystallization process to form the glass–ceramic.

Brazil is the world's largest producer of alcohol and sugar from sugarcane. In view of the strong national demand and the great interest shown by industrialized countries for ethyl alcohol, there is a current race in Brazil for the implementation of a substantial number of factories for the production of sugar and alcohol. The estimated 2007/2008 sugarcane harvest[8] is 528 Mt to produce sugar (49.47%) and alcohol (50.53%). The sugarcane stalks are crushed to extract their juice and the fibrous residue remaining is named bagasse. Currently, sugarcane bagasse is burned in boilers to produce steam, which is utilized in the factory processes and also to power turbines for the production of electrical energy, which supplies the factory energy needs with the excess being commercialized in the region. The volume of ash that will be produced in this harvest is approximately 3.2 Mt (1000 kg cane→250 kg bagasse→6 kg ash).

The crystallization of glass to make glass–ceramics consists of two steps, the nucleation and the growth stages. In the first stage, small stable volumes of product phase (crystalline) are formed, generally at preferential sites (interfaces or on the free surface) of the glass precursor. Often, internal nucleation or bulk nucleation is required, and the composition of the initial batch is selected to contain species that increase this form of nucleation. These species are called nucleating agents and can be metallic (i.e., Au, Ag, Pt, and Pd) or nonmetallic (i.e., TiO_2, P_2O_5, and fluorides). The rate of nucleation is strongly dependent on temperature, and once the stable nuclei are formed, the growth of the crystal begins. Growth involves the transport of matter, that is, the movement of atoms/molecules of glass through the glass/crystal interface and to the inside of the crystal. The driving force for this process is the difference in the free energy, ΔG_v, between the vitreous and crystalline states. The transport of atoms/molecules through the interface is thermally activated with an associated energy of activation, ΔG_a. Models involving these two energies have been developed for rate of growth as a function of temperature.[9,10]

Höland and Beall[9] discussed the base glasses of the SiO_2–Al_2O_3–CaO system (wollastonite) suitable for producing glass–ceramics according to the mechanism of controlled surface crystallization. Conventional heterogeneous nucleating agents, such as TiO_2 and ZrO_2 are used in the process. A base glass is produced in the form of granular glass particles measuring 1–7 mm that are required for controlling surface crystallization. Glass–ceramics with a main

wollastonite crystal phase have been made from these base glasses according to the above mechanism. The most significant glass–ceramic for building applications is manufactured under the brand name Neoparies, which is produced on a large scale as a building material especially for interior and exterior walls. A basic composition must first be melted to produce a melt that is poured into water to produce a frit. After molding, the glass grains are sintered to a dense monolithic glass by heat treatment. At temperatures above approximately 950°C, controlled surface crystallization of β-wollastonite ($CaO{\cdot}SiO_2$) begins at the boundary of the former glass grains. At 1000°C, wollastonite grows in needlelike form from the surface of the glass toward the interior of the glass grain, without crossing boundaries with neighboring glass particles. With heat treatment at 1100°C for 2 h, controlled surface crystallization of β-wollastonite for the production of finished glass–ceramic sheets ends. During this heat treatment, however, the crystallized boundaries join together to form large crystal needles with lengths of 1–3 mm. The boundaries of the base glass grains are virtually indiscernible in the glass–ceramic end product. However, more opaque β-wollastonite of a granular crystallographic morphology is produced if the β-wollastonite glass ceramics are heated to 1200°C rather than 1000°C.

According to Navarro,[11] this calcium metasilicate shows two different crystalline modifications: α-wollastonite (or pseudowollastonite) and β-wollastonite. The first corresponds to the stable form above 1180°C and thus appears in the shape of spheres or of aggregated large-sized crystals in glass masses cooled very slowly. β-Wollastonite is found more frequently at lower temperatures, and appears preferentially in the form of needles, prisms, or ribbons. Wollastonite ($CaSiO_3$) is a single chain silicate (*pyroxenoid*) with several polytypes. The high-temperature stable α-wollastonite occurs at T>1125°C.[12,13]

The study of the kinetics of crystallization based on the so-called Johnson–Mehl–Avrami–Kolmogorov (JMAK) model, in different materials by differential scanning calorimetry (DSC) and differential thermal analysis (DTA), has been widely discussed in the literature.[14–30] Various models have been proposed to determine kinetics parameters for nonisothermal conditions. These include the Ligero,[20] Kissinger,[21] and Matusita[22] methods. These models have been used in studies on the kinetics of glass crystallization for various glass–ceramic systems;[23–30] in the development of glass–ceramics from residues[1,2,5,6,14,31] and to study the crystallization of mullite from different materials,[16,19,32,33] among others.

For many transformations in the solid state, dependence of crystallization in relation to time is the same, that is, a sigmoidal curve results when the crystallized fraction is plotted as a function of the time. Mathematically, the crystallized fraction at time t, with the velocity of crystallization constant, is expressed by the JMAK equation as follows:

$$x(t) = 1 - \exp[(-kt)^n], \quad (1)$$

where n is the Avrami exponent, which describes the mechanism of crystallization and provides qualitative information on the nature of the processes of nucleation and growth of the crystals, this parameter varying between 0.5 and 4.

Taking the logarithm of the crystallization rate (dx/dt), an expression (Eq. (2)) is obtained that establishes a linear relationship between the logarithm of dx/dt and the inverse absolute temperature,[20]

$$\ln\left(\frac{dx}{dt}\right) = \ln[k_o f(x)] - \frac{E}{RT} \quad (2)$$

where, k_o is the frequency factor, f is a function of the crystallized fraction (x) and Avrami exponent (n), E is the activation energy, R is the ideal gas constant, and T is the isothermal temperature in Kelvin. This expression establishes that, for that interval of values of the crystallized fraction in which $f(x)$ is constant, there is a linear relationship between ln(dx/dt) and the absolute temperature inverse.[18]

The Kissinger method[21] is another kinetic approach used to analyze DTA data:

$$\ln\left(\frac{\phi}{T_p^2}\right) = -\frac{E}{RT_p} + \text{constant}, \quad (3)$$

where T_p is the peak crystallization temperature and φ is the DTA heating rate. A modified form of this equation was proposed by Matusita and Sakka[22]:

$$\ln\left(\frac{\phi}{T_p^2}\right) = -\frac{mE}{RT_p} + \text{constant} \quad (4)$$

where m is a numerical factor depending on the dimensionality of crystal growth. The values of $n$and m for various crystallization mechanisms obtained by Matusita *et al.* are shown in the work of Romero *et al.*[19]

In the present study, we applied the methods of Ligero, Kissinger, and Matusita, to study the kinetics of crystallization of glasses obtained with sugarcane bagasse ash as the source of silica.

II. Experimental Procedure

The bottom ash used in this work was collected in a sugar/alcohol factory from Presidente Prudente, Brazil. Before its use, the ash was hand crushed, sieved (18 mesh, 1 mm) and ground (400 rpm, 10 min) using a planetary steel ball mill (RETSCH, model PM100). Small amounts of

powdered ash were sent for chemical analysis (X-ray fluorescence [XRF]) and to identify crystalline phases (X-ray diffraction [XRD]). $CaCO_3$ and Na_2CO_3 of reagent grade were used as source of CaO and Na_2O, respectively.

A 100 g batch composition containing 49.1 g of ash, 45.8 g of CaO and 5 g of Na_2O was mixed and homogenized. The batch was heated at 10°C/min and melted in an alumina crucible at 1450°C for 1 h. Afterward, the melt was poured into water to produce a glass frit. The chemical composition of the frit was determined by XRF analysis. To determine the crystallization behavior of the glass, both a powder (<63 μm) and a monolithic glass sample were analyzed by thermal analysis (DTA/TG—SETARAM Labsys, Caluire, France) from room temperature to 1400°C at a heating rate of 50°C/min. The DTA scans were conducted in flowing air, platinum crucibles, and calcined Al_2O_3 as reference. All the DTA curves were normalized with respect to the sample weight. The kinetic study by nonisothermal method was performed on powder samples (<63 μm) from 20° to 1300°C and heating rates of 5°, 10°, 20°, 30°, 40° and 50°C/min.

To study the development of the crystalline phases, powder samples (<63 μm) were crystallized at different temperatures (750°, 800°, 830°, 860°, 900° and 970°C) at a heating rate of 50°C/min and held for 15 min. After this time, each sample was taken out the oven and cooled to room temperature. Phase identification was carried out by XRD (Philips X'PERT MPD Almelo, the Netherlands) using Cu*K*α radiation and operating at 50 kV and 30 mA. For XRD, powder samples (sieved <60 μm) were scanned in the 5°–60° (2θ) interval at a scanning speed of 0.5°/min.

III. Results and Discussion

(1) Chemical Analysis

Table I shows the chemical analyses by XRF of the sugarcane bagasse ash and derived glass frit. The major component of the ash is SiO_2, and among the minor components K_2O show the highest concentration. This composition differs from that reported in a previous study[34] due to differences in the type of sugarcane and, principally, in the soils where it was harvested. The Al_2O_3amount in the glass is incompatible with the ash composition, indicating a contamination from the alumina crucible. Other chemical elements, such as nucleating agents, are present in low amounts. X-ray diffraction of the ash showed that quartz is the major phase (Fig. 1).

Table I. Ash and Glass Chemical Compositions by X-Ray fluorescence (wt%)

Oxides	**Ash**	**Glass**
SiO_2	89.61	42.38
Al_2O_3	1.62	3.10
Fe_2O_3	1.33	0.93
Na_2O	—	4.72
K_2O	3.54	0.84
CaO	1.01	47.03
MgO	0.98	0.43
TiO_2	0.29	0.11
P_2O_5	1.37	0.20
SO_2	0.05	0.06
Cr_2O_3	0.08	0.13
SrO	0.01	0.02
BaO	0.05	0.04
Total	99.94	99.99

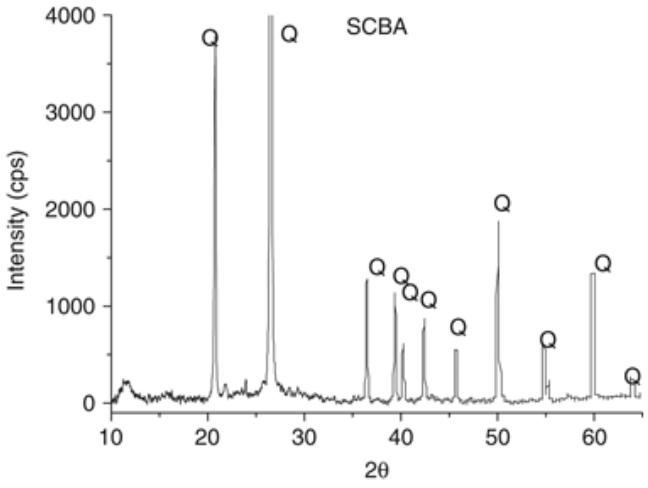

Figure 1. X-ray diffraction pattern of the sugar-cane bagasse ash (Q, Quartz).

(2) Thermal Analysis (TG/DTA)

The TG curve recorded on sugarcane bagasse ash during heating up to 1400°C show a small loss of mass (2%) indicating a low concentration of volatiles (moisture, carbonates, and charcoal).

DTA results for powder (<63 μm) and monolithic sample are shown in Fig. 2. The decrease in particle size leads to both a shift of the maximum of the exothermic peak to a lower temperature and an increase in the crystallization peak height. Considering that crystallization peak height is proportional to the number of nuclei formed in the glass, the difference in the results to both samples (Fig. 2) implies that surface crystallization plays a major role in the crystallization of the glass, in agreement with Li and Mitchell[35] who observed in calcium aluminate glasses that the crystallization peak height decreases with increasing particle size suggesting that the particles crystallize primarily by surface crystallization. Ray *et al.*[36] also have demonstrated this effect in different types of glasses when surface crystallization is the dominant mechanism.

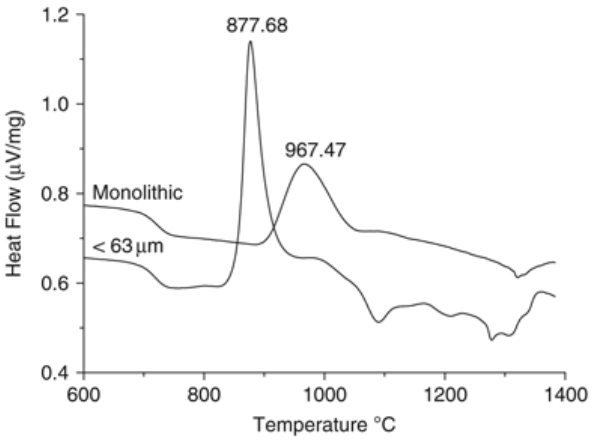

Figure 2. Differential thermal analysis curves of the glass powder (<63 μm) and monolithic sample (50°C/min).

The endothermic peak at around 1075°C indicates the formation of a liquid phase or the transition of 1 T to 2M-wollastonite.[13]

(3) XRD

Frit-sintered glass–ceramics crystallized at seven different temperatures for 15 and 60 min exhibited different XRD patterns indicating their crystalline phase development during thermal treatment, as shown in Fig. 3.

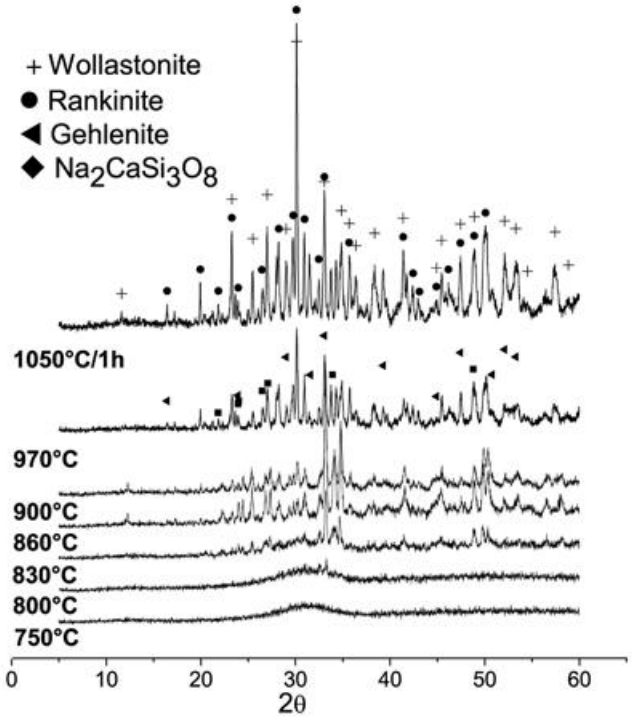

Figure 3. X-ray diffraction patterns of powder glass after heat treatment at 750°–970°C for 15 min and at 1050°C for 1 h. (• wollastonite $CaSiO_3$, ▪ rankinite $Ca_3Si_2O_7$, ♦ sodium-calcium silicate $Na_2CaSi_3O_8$, ○ gehlenite $Ca_2(Al(AlSi)O_7$, ↓ calcium-aluminum silicate $Ca_2Al_2SiO_7$).

At 750°C, no XRD peaks are observed, indicating an amorphous (glass) material. At 800°C some low intensity peaks indicate the onset of the crystallization process. From 830° to 970°C, the development of three major phases is observed: rankinite ($Ca_3Si_2O_7$), wollastonite ($CaSiO_3$) and a calcium–aluminum silicate ($Ca_2Al_2SiO_7$). Rankinite shows the more intense XRD peaks up to 900°C, and after that wollastonite exhibits more intense peaks. At higher temperatures (>900°C) the calcium–aluminum silicate disappears, and two new phases occur: gehlenite ($Ca_2(Al(AlSi)O_7$) and sodium–calcium silicate ($Na_2CaSi_3O_8$). The sample heated at 1050°C for 1 h shows an increase in the intensity of the XRD peaks and confirms wollastonite as the major phase. The DTA data did not detect this phase development and show one exothermic peak, suggesting that the crystallization of these phases is simultaneous and/or it occurs in a narrow

sequential process. Fan *et al.*[37] investigated the crystallization process of $CaSiO_3$ gel doped with Eu^{3+} and, under all conditions, rankinite seems to be the precursor of wollastonite, as observed in this work.

Mazzucato & Gualtieri[13] studied *in situ* crystallization kinetics of wollastonite polytypes in the CaO–SiO_2 (1:1 ratio) system and observed that 1T-wollastonite forms first and progressively transforms into an intermediate 1Td-wollastonite disordered form. Both phases in turn transform into 2M-wollastonite polytype, which is the high-temperature stable wollastonite formed at$T$>1125°C. As the sugarcane bagasse ash is not a pure material the phase peak positions are better adjusted to the 2M-wollastonite (75–1395) and para-wollastonite (72–2297). Moreover, the presence of other chemical elements changes the DTA peak positions and the simultaneous crystallization of other phases at once with wollastonite change the DTA crystallization peak intensity.

(4) Kinetics

Figure 4 depicts part of the DTA curves recorded for powder samples (<63 μm) at six different heating rates from room temperature to 1300°C. The glass transition (at around 710°C) is followed by a single exothermic crystallization peak. Although the XRD data showed that more than one phase was involved in crystallization, only one crystallization peak was seen here.

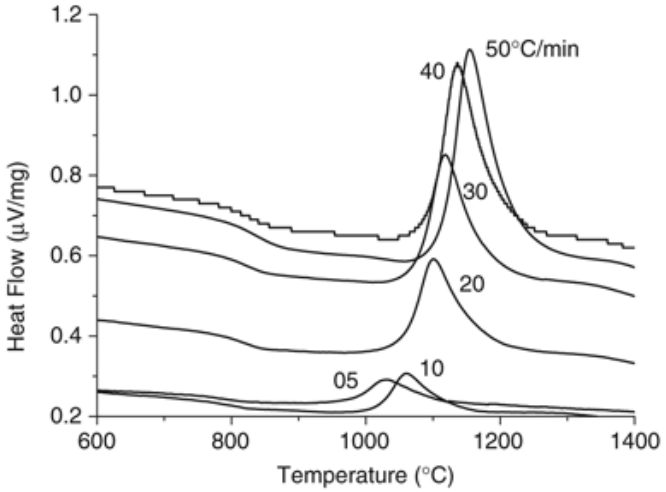

Figure 4. Differential thermal analysis curves for the glass (powder <63 μm) at different heating rates (5°, 10°, 20°, 30°, 40° and 50°C/min).

The kinetic parameters were calculated using the Ligero method[20] in which the crystallized fraction interval at which the model is constant was taken into account (Eq. (2)). Figure 5 shows the plot of ln(dx/dt) with the inverse absolute temperature (1/T) at the same value of crystallized fraction (x) for the different heating rates. It is seen that this plot is linear (r>0.99) in the range$x$=0.10–0.70 giving an average activation energy of 378±13 kJ/mol for glass crystallization. The Avrami parameter, n, was obtained by selecting many pairs of x_1 and x_2 that satisfy the condition $\ln[k_o f(x_1)]=\ln[k_o f(x_2)]$. These pairs of crystallization fractions x were taken from the data table, to each heating rate. Each data table was duplicated and the x values were obtained comparing them in the two tables, one from the beginning to the end with the other from the end to the beginning. The average parameter value using this method is 1.50.

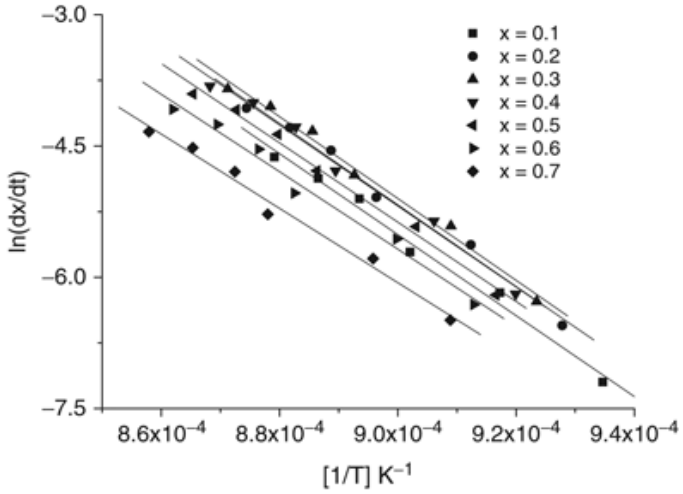

Figure 5. Plot of ln(dx/dt) vs. 1/T at the same crystallized fraction (x), using Ligero method.[18]

Figure 6 shows the plot of $\ln[\varphi/T_p^2]$ versus $1/T_p$, using the Kissinger method (Eq. (3)). The activation energy calculated from the slope (r=0.99) of this plot is 374±10 kJ/mol, which is in good agreement with that estimated by the Ligero method (378±13 kJ/mol). Using the Matusita equation (Fig. 7), n from the Ligero equation, and activation energies (E_a) from Ligero and Kissinger methods, the numerical factor m obtained was 1.51 (for Ligero E_a) and 1.53 (for Kissinger E_a). Both parameters (n and m) have values close to 1.5, which is an indication of a three-dimensional growth of crystalline phases with polyhedron-like morphology. These results also indicate that bulk nucleation is the dominant mechanism and that crystal growth is controlled by diffusion from a constant number of nuclei. The presence of a mineralizer agent (Na_2CO_3) or flux and small content of nucleating agents in the glass can favor bulk nucleation in

the kinetic process.[7] However, it is important to point out that kinetic results are in disagreement with the previous results taken from DTA curves (Fig. 2), which indicate that crystallization of the powder glass sample occurs through a surface mechanism. Taken together, these results suggest that the early stage of surface crystallization occurs through a three-dimensional growth of crystals, which will then transform to one-dimensional growth.

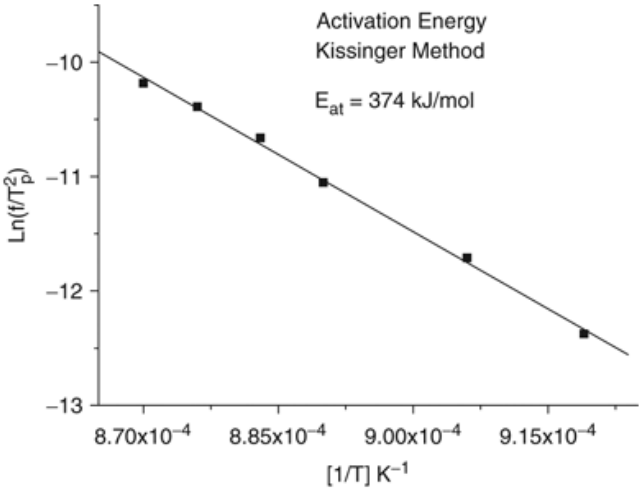

Figure 6. Plot for determination of the activation energy according to Kissinger method.[19]

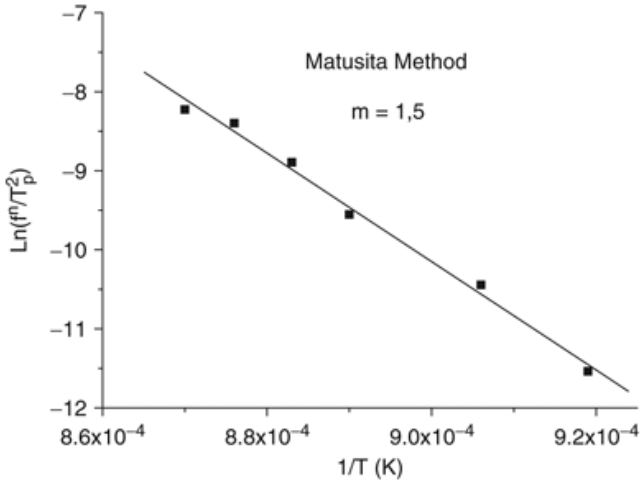

Figure 7. Plot for determination of the activation energy according to Matusita method.[20]

This result has been confirmed by scanning electron microscopy (SEM). Thus, Fig. 8 shows the microstructure observed by SEM on the glass sintered at 1050°C for 1 h. It is clearly observed a crystallization shell consisted of spherulitic crystals (three-dimensional), which induce the development of linear fiber-like crystals aggregations. This result is in agreement with Karamanov *et al.*,[38] who studying formation of diopside crystals via surface crystallization observed that during the initial stage of crystallization a three-dimensional growth takes place and later on, one-dimensional growth inward the grain is possible. This modification in the crystallization mechanism will change the reaction order, *n*.

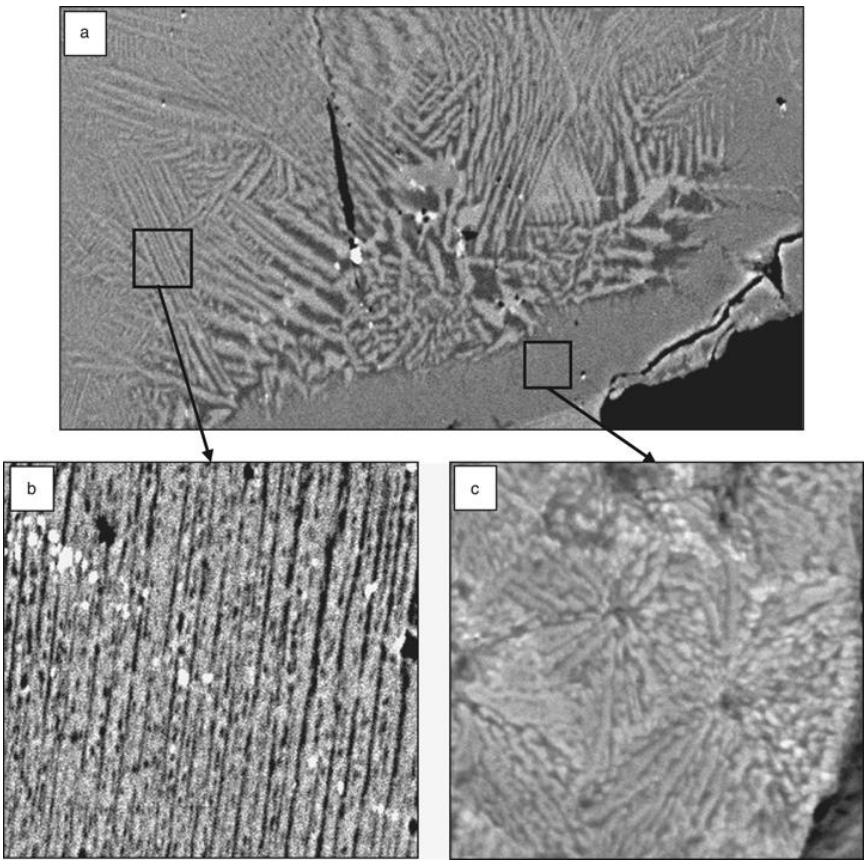

Figure 8. Microstructure observed by scanning electron microscopy on glass particles after treatment at 1050°C/1 h: (a) general aspect, (b) one-dimensional growth inward the grain and (c) three-dimensional growth shell at the grain particle.

Both crystallization mechanisms can occur simultaneously and one of them dominates over the other in different stages (or times) of the reaction. The broad crystallization peak at 5°C/min

indicates surface crystallization. The Avrami parameter *n* associated to it (using Augis–Bennett equation)[39] is 1.64 (close to 1.0) indicating surface crystallization. To the others crystallization peaks obtained at higher heating rates the Avrami parameter is higher than 2, close to 3, indicating internal or three-dimensional transformation (Table II).[36] This change of parameter *n*, between 1 and 3, indicates that both mechanisms occur simultaneously. Our data shows that both mechanisms occur, according to Fig. 2 the surface crystallization is predominant and according to kinetic data the internal crystallization is the dominant mechanism. Then we conclude that the initial stage of surface crystallization occurs through a three-dimensional growth of crystals.

Table II. Calculated Values of Avrami Parameter[39]

Heating rate	Peak temperature (K)	Width at half-max	n
5°C/min	1088	40	1.64
10	1103	29	2.32
20	1123	33	2.11
30	1132	30	2.36
40	1141	29	2.48
50	1150	30	2.44
Mean value			2.22

The ash mineralogical composition makes it difficult to compare these kinetic data with other findings about the CaO–SiO_2 system with wollastonite formation.[9,13,40–42] Heterogeneous nucleation occurs due to the minor chemical elements in the ash that can interfere with the kinetic process shifting the crystallization peaks and the crystal growth rate of the glass.[9] Rizkalla *et al.*[40] studied the CaO–SiO_2–Na_2O–P_2O_5 system with six different compositions. The activation energy of crystallization ranged from 196 to 782 kJ/mol, and one of the compositions gave an activation energy of 330 kJ/mol and *n*=1.5, very close to our results but with surface crystallization. According to Mazzucato and Gualtieri,[13] it is possible that the use of mineralizers favored the crystallization of the wollastonite phase in Rizkalla' work. These authors studied the (1:1) CaO–SiO_2system and obtained activation energy values of 520 and 590 kJ/mol for wollastonite 1T (triclinic structure) and of 430 and 360 kJ/mol to 1Td crystallizations. Their data show that in the kinetics of 1T-wollastonite formation the reaction is

phase boundary-controlled with a constant or decelerating nucleation rate and one-dimensional growth at lower temperatures (T<875°C). According to them, this is in contrast with earlier preliminary observations indicating a reaction controlled by diffusion.[12]

IV. Conclusions

The results obtained in this investigation show that it is possible to use sugarcane bagasse ash to produce useful glass–ceramic products.

For this ash chemical composition and glass formulation, two calcium silicates (wollastonite and rankinite) and one Na–Ca-silicate are the principal phases formed. Wollastonite is the major phase in crystallization at T>970°C, and below this temperature there is a predominance of rankinite.

The glass transition temperature is around 710°C. The DTA data show one exothermic peak (around 870°C), suggesting that the crystallization of these phases is simultaneous and/or much closer sequential processes.

The crystallization activation energies calculated by the Kissinger and Ligero methods are equivalent: 374±10 and 378±13 kJ/mol.

DTA curves suggest that surface crystallization plays a major role in the crystallization of the powder sample. However, growth morphology parameters have equal values n=m=1.5 indicating that bulk crystallization is the dominant mechanism in this crystallization process, where there is a three-dimensional growth of crystals with polyhedron-like morphology controlled by diffusion from a constant number of nuclei. Taken together, these results suggest that the initial stage of surface crystallization occurs through a three dimensional growth of crystals.

Acknowledgments

One of the authors (S. R. Teixeira) is greatly indebted to FAPESP (04368-4/08), to UNESP/PROPE-SANTANDER post-doc program for the scholarship and to ICCET/CSIC for the laboratories and materials accessibility. We are also grateful to Dr Ma. S. Hernandez Crespo for assistance in the development of this work and to Pilar Díaz Díaz for technical support.

References

1 M. Romero, R. D. Rawlings, and J. Ma. Rincón, "Development of a New Glass–Ceramic by Means of Controlled Vitrification and Crystallization of Inorganic Wastes from Urban Incineration," J. Eur. Cer. Soc., 19, 2049–58 (1999).

2 A. M. F. Barbieri, I. Lancelloti, C. Leonelli, J. Ma. Rincón, and M. Romero, "Crystallization of (Na_2O–MgO)–CaO–Al_2O_3–SiO_2 Glassy Systems Formulated from Waste Products," J. Am. Cer. Soc., 8 [10] 2515–20 (2000).

3 L. Barbieri, I. Lancelloti, T. Manfredini, G. C. Pellacani, J. Ma. Rincón, and M. Romero, "Nucleation and Crystallization of New Glasses Obtained from Fly Ash Originating from Thermal Power Plants," J. Am. Cer. Soc., 84, 1851–8 (2001).

4 M. Romero and J. Ma. Rincón, "El proceso de vitrificación/cristalización controlada aplicado al reciclado de residuos industriales inorgánicos," Bol. Soc. Esp. Ceram. Vidrio, 39, 155–63 (2000).

5 M. Romero, J. Ma. Rincón, R. D. Rawlings, and A. R. Boccacinni, "Use of Vitrified Urban Incinerator Waste as Raw Material for Production of Sintered Glass–Ceramics," Mater. Res. Bull., 36, 383–95 (2001).

6 E. Bernardo, R. Castellano, and S. Hreglich, "Sintered Glass–Ceramics from Mixtures of Wastes," Cer. Int., 33, 27–33 (2007).

7 R. D. Rawlings, J. P. Wu, and A. R. Boccaccini, "Glass–Ceramics: Their Production from Wastes—A Review," J. Mater. Sci., 41, 733–61 (2006).

8 CONAB—Companhia Nacional de Abastecimento, "Acompanhamento da Safra Brasileira Cana-de-Açucar 2007/2008" (Accompaniment of the Brazilian sugar-cane 2007/2008 harvest), Ministry of Agriculture—Brazil, http://www.conab.gov.br/conabweb/download/safra/3lev-cana.pdf

9 W. Höland and G. Beall, Glass—Ceramic Technology. The American Ceramic Society, Westerville, OH, 2002.

10 H. Scheel and T. Fukuda, Crystal Growth Technology. John Wiley & Sons Ltd, Chichester, 2004.

11 J. M. F. Navarro, "El Vidrio" (The Glass), Consejo Superior de Investigaciones Cientificas—CSIC, Sociedad Española de Cerámica y Vidrio, Madrid, España, (2003).

12 A. F. Gualtieri, E. Mazzucato, C. C. Tang, and B. Cernik, "Crystallisation Kinetics and Phase Relations of Wollastonite by Real Time Synchrotron Powder Diffraction," Mater. Sci. Forum, 321–4, 224–229 (2000).

13 E. Mazzucato and A. F. Gualtieri, "Wollastonite Polytypes in the CaO–SiO_2 System," Phys. Chem. Miner., 27, 565–74 (2000).

14 M. Romero, J. Kovacova, and J. M. Rincón, "Effect of Particle Size on Kinetic Crystallization of an Iron-Rich Glass," J. Mater. Sci., 43, 4135–42 (2008).

15 Y.-F. Chen, M.-C. Wang, and M.-H. Hon, "Phase Transformation and Growth of Mullite in Kaolin Ceramics," J. Eur. Cer. Soc., 24, 2389–97 (2004).

16 N. F. Nascimento, N. T. Silva, and G. P. Thim, "Estudo da cinética de cristalização de mulita". Instituto de Tecnologia Aeronáutica—ITA, Departamento de Química, São José dos Campos—SP, Brasil. http://www.bibl.ita.br/ixencita/artigos/FundNatalia.pdf, (2004).

17 A. C. Faleiros, T. N. Rabelo, G. P. Thim, and M. A. S. Oliveira, "Kinetics of Phase Change," Mat. Res., 3 [3] 51–60 (2000).

18 M. J. Starink and A. M. Zahra, "An Analysis Method for Nucleation and Growth Controlled Reactions at Constant Heating Rate," Thermochim. Acta, 292, 159–68 (1997).

19 M. Romero, J. Martin-Márquez, and J. Ma. Rincón, "Kinetic of Mullite Formation from a Porcelain Stoneware Body for Tiles Production," J. Eur. Cer. Soc., 26, 1647–52 (2006).

20 R. A. Ligero, J. Vázques, P. Villares, and R. Jiménez-Garay, "A Study of the Crystallization Kinetics of Some Cu–As–Te Glasses," J. Mater. Sci., 26, 211–5 (1991).

21 H. E. Kissinger, "Variations of Peak Temperature with Heating Rate in Differential Thermal Analysis," J. Res. Nat1. Bur. Stnd., 57, 217–21 (1956).

22 K. Matusita and S. Sakka, "Kinetic-Study on Crystallization of Glass by Differential Thermal-Analysis: Criterion on Application of Kissinger Plot," J. Non-Cryst. Sol., 38–9, 741–6 (1980).

23 C. Oprea, C. Stan, E. Rotiu, and C. Popescu, "Non-Isothermal Crystallization of Cordierite Glasses," J. Therm. Anal. Cal., 56, 611–5 (1999).

24 S. P. Hwang and J. M. Wu, "Effect of Composition on Microstructural Development in MgO–Al_2O_3–SiO_2 Glass–Ceramics," J. Am. Cer. Soc., 84, 1108–12 (2001).

25 P. Wange, T. Höche, C. Rüssel, and J. D. Schnapp, "Microstructure-Property Relationship in High-Strength MgO–Al_2O_3–SiO_2–TiO_2 Glass–Ceramics," J. Non-Cryst. Sol., 298, 137–45 (2002).

26 V. C. S. Reynoso, K. Yukimitu, T. Nagami, C. L. Carvalho, J. C. S. Moraes, and E. B. Araújo, "Crystallization Kinetics in Phosphate Sodium-Based Glass Studied by DSC Technique," J. Phys. Chem. Sol., 64, 27–30 (2003).

27 L. Wondraczek, J. Deubener, S. T. Misture, and R. Knitter, "Crystallization Kinetics of Lithium Orthosilicate Glasses," J. Am. Cer. Soc., 89 [4] 1342–6 (2006).

28 G. H. Chen, "Effect of Replacement of MgO by CaO on Sintering Crystallization and Properties of MgO–Al_2O_3–SiO_2 System Glass–Ceramics," J. Mater. Sci., 42 [17] 7239–44 (2007).

29 C. S. Ray, T. Zhang, S. T. Reis, and R. K. Brow, "Determining Kinetic Parameters for Isothermal Crystallization of Glasses," J. Am. Cer. Soc., 90 [3] 769–73 (2007).

30 A. Goel, E. R. Shaaban, F. C. L. Melo, M. J. Ribeiro, and J. M. F. Ferreira, "Non-Isothermal Crystallization Kinetic Studies on MgO–Al_2O_3–TiO_2 Glass," J. Non-Cryst. Sol., 353, 2383–91 (2007).

31 C. N. Djangang, A. Elimbi, U. C. Melo, G. L. Lecomte, C. Nkoumbou, J. Soro, J. P. Bonnet, P. Blanchart, and D. Njopwouo, "Sintering of Clay–Chamote Ceramic Composites for Refractory Bricks," Cer. Int., 34 [5] 1207–13 (2008).

32 R. R. Monteiro, A. C. S. Sabioni, and G. M. Costa, "Preparação de mulita a partir do mineral topázio," Cerâmica, 50, 318–23 (2004).

33 A. L. Campos, E. Y. Kawachi, T. C. Oliveira, and G. P. Thim, "Mullite Crystallization Mechanism Obtained from Kinetic Parameters Determination for Seeded and Non-Seeded Gel," Mater. Sci. Eng. B, 122 p. 169–73 (2005).

34 S. R. Teixeira, A. E. Souza, G. T. A. Santos, A. F. V. Peña, and A. G. Miguel, "Sugar Cane Bagasse Ash (SCBA) as a Potential Quartz Replacement in Red Ceramic," J. Am. Cer. Soc., 91, 1883–7 (2008).

35 W. Li and B. S. Mitchell, "Nucleation and Crystallization in Calcium Aluminate Glasses," J. Non-Cryst. Sol., 255, 199–207 (1999).

36 C. S. Ray, Q. Yang, W. Huang, and D. E. Day, "Surface and Internal Crystallization in Glasses as Determined by Differential Thermal Analysis," J. Am. Cer. Soc., 79, 3155–60 (1996).

37 X. Fan, M. Wang, Z. Hong, and G. Qian, "The Process of Crystallization of CaSiO3 Gel and the Luminescence of Eu[3]+ Ions in Gel-Derives Crystals," J. Phys: Condens. Matt., 9, 3479–86 (1997).

38 A. Karamanov, R. Pascova, I. Avramov, and I. Gutzow, "Determination of Avrami Parameter in the Case of Non-Isothermal Surface Crystallization of Powdered Glasses"; pp. 26–30 in 16th International Conference of Glass and Ceramics Proceedings, Varna, Bulgaria, 2008.

39 J. A. Augis and J. E. Bennett, "Calculation of the Avrami Parameters for Heterogeneous Solid-State Reactions using a Modification of the Kissinger Method," J. Therm. Anal., 13, 283–92 (1978).

40 A. S. Rizkalla, D. W. Jones, D. B. Clarke, and G. C. May, "Crystallization of Experimental Bioactive Glass Compositions," J. Biom. Mater. Res., 32, 119–24 (1996).

41 L. V. Morais and A. T. Fonseca, "Kinetics of Isothermal Solid State Reaction of β-Wollastonite Synthesis from Natural Raw Materials," Br. Cer. Trans., 96 [2] 61–5 (1997).

42 L. Gránásy, T. Wang, and P. F. James, "Kinetics of Wollastonite Nucleation in CaO–SiO_2 Glass," J. Chem. Phys., 108, 7317–26 (1998).